2014 IEEE International Conference on Acoustic, Speech and Signal Processing (ICASSP)

EFFECT OF PHASE NOISE ON DIGITAL SELF-INTERFERENCE CANCELLATION IN WIRELESS FULL DUPLEX

Shihai Shao, Xin Quan, Ying Shen, and Youxi Tang

National Key Lab of Science and Technology on Communications,
University of Electronic Science and Technology of China, 611731 Chengdu, China

ABSTRACT

Oscillator phase noise in a full duplex radio causes the mismatch between the self-interference (SI) signal and the cancelling signal, and thus degrades performance of the digital SI cancellation (SIC). In this paper, we analyze the effect of phase noise on digital SIC in wireless full duplex. We consider an OFDM-based full duplex radio corrupted by the phase noise at both the transmitter and the receiver, which are modeled as independent Wiener processes. A closed-form expression for the cancellation ability of a common digital SIC scheme is derived, in terms of the interference-to-noise ratio (INR), the SI subcarrier spacing and the oscillator's 3dB coherence bandwidth. The theoretical analysis and simulations reveal that the digital SIC ability degrades with the increase of the ratio of the oscillator's 3dB coherence bandwidth to the signal bandwidth, which determines the upper bound of the digital SIC ability.

Index Terms— Digital self-interference cancellation, full duplex, phase noise

1. INTRODUCTION

A full duplex radio is defined as a radio frequency (RF) transceiver that can transmit and receive signals at the same time and the same frequency, and thus has twice as high spectral efficiency as a half-duplex radio [1]. Motivated by its advantages, full duplex has attracted much research interest [2, 3, 4, 5] and some experimental verifications have been made in recent years[6, 7, 8, 9, 10]. In a full duplex radio, a strong self-interference (SI) occurs at the receiver [1], thus self-interference cancellation (SIC) is an essential part in full duplex design. There are three basic approaches of SIC, i.e., antenna SIC, analog SIC, and digital SIC [1], which are usually combined and deployed sequentially in practice in order to suppress the strength of SI as much as possible.

Ideally, the SIC could reduce the power of SI to the noise floor by employing the knowledge of SI [5]. However, it is

This work was supported by the National Natural Science Foundation of China (61271164, U1035002/L05, 61001087, 61101034), the National major projects (2014ZX03003001-002, 2012ZX03003010-003, 2011ZX03001-006-01) and Open Research Fund of the Academy of Satellite Application.

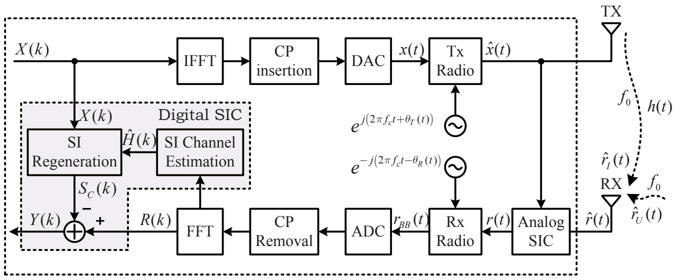

Fig. 1. Systematic scheme of digital SIC with phase noise.

hard to eliminate the SI completely, i.e., residual SI always exists in most of the designs [6, 7, 8, 9, 10]. For instance, in [7], even after the antenna, analog and digital SICs, the power of residual SI is 15 dB above the thermal noise floor, while in [10], it is only 1 dB above the noise floor. In practical full-duplex radio, the residual SI power is determined not only by the cancellation scheme, but also by the hardware and implementation imperfections [11], such as the phase noise at the transmitter and the receiver, power amplifier non-linearity and quantization noise. Among these imperfections, phase noise is one of the most important factors that cause performance degradation of the SIC [5].

Recently, studies have been conducted to investigate the effect of phase noise on full duplex radios [4, 5, 11, 12, 13]. The effect of phase noise on the signal-to-interference and noise ratio (SINR) and the transmission rate was analyzed using different phase noise models [11, 12, 13], while the effect on SIC performance was not clearly concluded. Furthermore, in [4, 5], the impact of phase noise on the amount of cancellation of analog and digital SIC was studied. It is shown that the amount of cancellation, which combines analog cancellation and digital cancellation, depends on the inverse of the variance of phase noise. These papers analyzed the effect of phase noise on the residual SI, without specifying the SI signal format and the SI channel estimation scheme. Besides, the SI channel estimation error caused by phase noise and the effect of the SI bandwidth on digital SIC ability are remain unconsidered.

In this paper, we consider an OFDM-based full duplex

978-1-4799-2893-4/14/$31.00 ©2014 IEEE

radio corrupted by phase noise at the transmitter and receiver , which are modeled as independent Wiener processes. Adopting a common digital SIC scheme [7, 8], we derive a closed-form expression for the digital SIC ability, in terms of the interference-to-noise ratio, the oscillator's 3dB coherence bandwidth and the SI subcarrier spacing. Simulations are also presented to evaluate digital SIC performance, which show that digital SIC ability degrades with the increase of the ratio of the oscillator's 3dB coherence band width to the subcarrier spacing.

2. SYSTEM MODEL

2.1. Signal Model

An OFDM-based full duplex radio with N_c subcarriers is shown in Fig. 1. A standard OFDM modulator transforms the digital frequency-domain symbols $\{X(k)\}_{k=0}^{N_c-1}$ into an analog baseband signal $x(t)$ which is then upconverted to RF band by the transmit oscillator signal $e^{j[2\pi f_c t+\theta_T(t)]}$ with the transmit phase noise $\theta_T(t)$ and the carrier frequency f_c. After a passband filter and a high-power amplifier (not shown in Fig. 1), the RF signal $\hat{x}(t)$ is transmitted to the far-end, and also received by the local receiver through a multipath channel whose impulse response is given by $h(t)$, becoming the SI signal $\hat{r}_I(t)$. In the local receiver, the received RF signal $\hat{r}(t)$ consists of the SI signal $\hat{r}_I(t)$, the desired signal $\hat{r}_U(t)$, and the white Gaussian noise $\hat{n}(t)$ with variance σ_N^2. After analog SIC which aims at cancelling some strong multipath SI [14], the received signal $\hat{r}(t)$ becomes $r(t)$ and downconverted to the baseband by the receive oscillator signal $e^{-j[2\pi f_c t-\theta_R(t)]}$ where $\theta_R(t)$ is the receive phase noise. The received baseband signal $r_{\mathrm{BB}}(t)$ is converted to the discrete frequency domain by applying sequentially the analog-to-digital, cyclic prefix (CP) removal, and discrete Fourier transform (DFT) operations to obtain$\{R(k)\}_{k=0}^{N_c-1}$, where the signal at the k-th subcarrier is

$$R(k) = R_I(k) + R_U(k) + N(k), \tag{1}$$

with $R_I(k)$, $R_U(k)$, and $N(k)$ the digital frequency-domain symbols of $r_I(t)$, $r_U(t)$, and $n(t)$ after analog-to-digital convertion, respectively.

Since the analysis is concentrated on the effect of phase noise on SIC, in the following we will only consider the SI symbols $\{R_I(k)\}_{k=0}^{N_c-1}$. Following the signal path, according to [15], we obtain the expression for the SI symbols as

$$R_I(k) = H(k)\delta_0 X(k) + H(k)\sum_{i=0,i\neq k}^{N_c-1}\delta_{i-k}X(i), \tag{2}$$

where

$$\delta_{i-k} = \frac{1}{N_c}\sum_{n=0}^{N_c-1} e^{j(\theta_T(n)+\theta_R(n))}e^{-j2\pi\frac{(i-k)n}{N_c}} \tag{3}$$

is the N_c-point DFT of the transmitter and the receiver phase noise. The discrete-time equivalents of $\theta_T(t)$ and $\theta_R(t)$ are given by $\theta_T(n)$ and $\theta_R(n)$, respectively. $\{H(k)\}_{k=0}^{N_c-1}$ is the frequency response of the discrete version of $h_c(t)$, which is the multipath channel impulse response after analog SIC.

Letting the SI symbol vector $\mathbf{R}_I = [R_I(0), \cdots, R_I(N_c-1)]^T$, the channel vector $\mathbf{H} = [H(0), \cdots, H(N_c-1)]^T$, and the transmit symbol vector $\mathbf{X} = [X(0), \cdots, X(N_c-1)]^T$, from (2), we have

$$\mathbf{R}_I = \mathbf{\Lambda}\mathbf{H}, \tag{4}$$

where $\mathbf{\Lambda} = diag\{\mathbf{\Delta}_1^T\mathbf{X}, \mathbf{\Delta_2^T}\mathbf{X}, \cdots, \mathbf{\Delta_{N_c-1}^T}\mathbf{X}\}$ and $\mathbf{\Delta}_k = [\delta_{-k}, \delta_{1-k}, \cdots, \delta_{N_c-1-k}]^T$.

Using (4), the substitution of (1) yields

$$\mathbf{R} = \mathbf{\Lambda}\mathbf{H} + \mathbf{R}_U + \mathbf{N}, \tag{5}$$

where $\mathbf{R} = [R(1), \cdots, R(N_c-1)]^T$, is the frequency domain received signal vector, $\mathbf{R}_U = [R_U(1), \cdots, R_U(N_c-1)]^T$, is the frequency domain desired signal vector, and $\mathbf{N} = [N(1), \cdots, N(N_c-1)]^T$ is the frequency domain noise vector.

2.2. Digital Self-Interference Cancellation

The digital SIC, as shown in Fig. 1, consists of three components: estimating the SI channel; using the SI channel estimate $\hat{H}(k)$ and the known transmit signal $X(k)$ to generate the SI digital symbols; and subtracting the regenerated SI symbols from the received symbols [7].

Denoting the N_c-dimensional channel estimate vector by $\hat{\mathbf{H}}$, according to [7], we have the regenerated vector $\mathbf{S}_c$ as

$$\mathbf{S}_c = \mathbf{X}_\Lambda\hat{\mathbf{H}}, \tag{6}$$

where $\mathbf{X}_\Lambda$ is an $N_c \times N_c$ diagonal matrix

$$\mathbf{X}_\Lambda = diag\{X(0), X(1), \cdots, X(N_c-1)\}. \tag{7}$$

After digital SIC, the residual self-interference vector $\mathbf{Y}_r$ is

$$\mathbf{Y}_r = \mathbf{R}_I - \mathbf{S}_c = \mathbf{\Lambda}\mathbf{H} - \mathbf{X}_\Lambda\hat{\mathbf{H}}. \tag{8}$$

The cancellation ability G(dB) is defined as

$$G = 10\lg\frac{E_I + \sigma_N^2}{E_r + \sigma_N^2} \tag{9}$$

with E_I, E_r, σ_N^2 the power of SI before cancellation, after cancellation, and the noise, respectively.

3. EFFECT OF PHASE NOISE ON SIC

In Section 2, we have introduced the method to regenerate the SI signal using the estimated SI channel vector $\hat{\mathbf{H}}$. In this section, we use the maximum likelihood estimator (MLE) to obtain $\hat{\mathbf{H}}$, and then analyze the effect of phase noise on SIC.

3.1. Channel Estimation with Phase Noise

We assume that pilots are multiplexed into the data stream, i.e., a total of N_p pilots $\{a(n)\}_{n=0}^{N_p-1}$ are uniformly inserted in the OFDM block at N_p known locations $\{i_n\}_{n=0}^{N_p-1}$ for the best performance [16].

We also assume that the channel variations are negligible over one data block, and we indicate with $\mathbf{h}_c = [h_c(0), h_c(1), \cdots, h_c(L-1)]^T$ the T_s-spaced samples of the overall channel impulse response (CIR) $h_c(t)$, where L is the number of channel taps. Then the SI channel vector $\mathbf{H}$ can be computed as

$$\mathbf{H} = \mathbf{F}\mathbf{h}_c, \tag{10}$$

where $\mathbf{F}$ is an $N_c \times L$ DFT matrix with entries $[\mathbf{F}]_{n,k} = e^{-j2\pi nk/N_c}$, $0 \le n \le N_c - 1$, $0 \le k \le L-1$.

Using pilots $\{a(n)\}_{n=0}^{N_p-1}$ and (1), (2), we have the received symbols at the pilot locations as

$$\begin{aligned} R(i_n) =& \delta_0 a(n) H(i_n) + H(i_n) \sum_{i=0, i\neq i_n}^{N_c-1} \delta_{i-i_n} X(i) \\ &+ R_U(i_n) + N(i_n) \end{aligned} \tag{11}$$

Rewriting these received symbols $\{R(i_n)\}_{n=0}^{N_p-1}$, the N_p-dimensional received vector at the pilot locations is obtained as

$$\mathbf{R}_{pl} = \delta_0 \mathbf{A}\mathbf{B}\mathbf{h}_c + \mathbf{M}\mathbf{B}\mathbf{h}_c + \mathbf{S}_{Upl} + \mathbf{N}_{pl}, \tag{12}$$

where $\mathbf{A}$ is a diagonal matrix $\mathbf{A} = diag\{a(0), \cdots, a(N_p-1)\}$, $\mathbf{B}$ is an $N_p \times L$ matrix with entries $[\mathbf{B}]_{n,k} = e^{-j2\pi k i_n/N_c}$, $0 \le n \le N_p - 1, 0 \le k \le L-1$. $\mathbf{M}$ is a diagonal matrix representing the intercarrier interference (ICI) introduced by phase noise, with entries

$$[\mathbf{M}]_{k,k} = \mathbf{\Delta}_{i_k}\mathbf{X} - \delta_0 X(i_k) = \sum_{i=0, i\neq i_k}^{N_c-1} \delta_{i-i_k} X(i), \tag{13}$$

and $\mathbf{S}_{Upl}$ and $\mathbf{N}_{pl}$ are the desired symbol vector and the noise vector at the pilot locations, respectively. The vector $\mathbf{N}_{pl}$ follows the Gaussian distribution with zero mean and covariance matrix $\mathbf{C}_{N_{pl}} = \frac{\sigma_N^2}{N_c}\mathbf{I}_{N_p}$, where $\mathbf{I}_{N_p}$ is the identity matrix of order N_p.

Assuming that pilot symbols are taken from a PSK constellation, i.e., $|a(n)| = E_s/N_c$, by premultiplying both sides of (12) by $\mathbf{A}^H$, dividing E_s/N_c and applying the MLE in [16], the SI channel estimation is derived as

$$\hat{\mathbf{H}} = \delta_0 \mathbf{H} + \frac{N_c}{N_p E_s}\mathbf{F}\mathbf{B}^H\mathbf{A}^H(\mathbf{M}\mathbf{B}\mathbf{h}_c\mathbf{S}_{Upl} + \mathbf{N}_{pl}). \tag{14}$$

Considering the case without phase noise, in [16], the estimation result becomes

$$\hat{\mathbf{H}}_0 = \mathbf{H} + \frac{N_c}{N_p E_s}\mathbf{F}\mathbf{B}^H\mathbf{A}^H\mathbf{N}_{pl}. \tag{15}$$

Comparing (14) and (15), we notice that, in an OFDM-based full duplex radio with phase noise, the channel estimation result is influenced by phase noise through the factor δ_0 and the ICI matrix $\mathbf{M}$.

3.2. Effect of Phase Noise on SIC

The power of the residual self-interference $\mathbf{Y}_r$ is computed as (assuming $E\{|X(n)|^2\} = E_s/N_c$ and $E\{X(n)X^*(k)\} = 0,\ n \neq k$)

$$\begin{aligned} E_r =& E\{||\mathbf{Y_r}||^2\} = E\{(\mathbf{\Lambda H} - \mathbf{X}_\Lambda\hat{\mathbf{H}})^H(\mathbf{\Lambda H} - \mathbf{X}_\Lambda\hat{\mathbf{H}})\} \\ =& \frac{E_s}{N_c}\sum_{i=0}^{N_c-1}\sum_{y=0,y\neq i}^{N_c-1} E\{|H(i)|^2\}E\{|\delta_{y-i}|^2\} + \frac{L(E_U+\sigma_N^2)}{N_p} \\ &+ \frac{LE_s}{N_p^2}\sum_{x=0}^{N_p-1}\sum_{y=0,y\neq i_x}^{N_c-1} E\{|H(i_x)|^2\}E\{|\delta_{y-i_x}|^2\}. \end{aligned} \tag{16}$$

where $E\{|\delta_x|^2\}$ can be computed as following.

Phase noise of two oscillators with the same parameters can be modeled well as a Wiener process [12] such that $\theta_T(n) - \theta_T(n-1)$ and $\theta_R(n) - \theta_R(n-1)$ are normally distributed with variance $\alpha = 4\pi f_{3\text{dB}}T_s$, where $\theta_T(n)$ is independent of $\theta_R(n)$. And T_s is the sampling interval. The quality of the oscillator is parameterized by $f_{3\text{dB}}$ which defines the 3dB coherence bandwidth of its power spectral density. According to (3), and applying Wiener process phase noise, we can compute $E\{|\delta_x|^2\}$ as

$$E\{|\delta_x|^2\} = \frac{\left\{2\Re\left[\frac{d_x^{N_c+1} - (N_c+1)d_x + N_c}{(d_x-1)^2}\right] - N_c\right\}}{N_c^2}, \tag{17}$$

where $d_x = e^{-\alpha - j2\pi x/N_c}$ [17].

It is found that the summation $\sum_{y=o,y\neq i}^{N_c-1}|\delta_{y-i}|^2$ in (16) does not depend on the index i [15], i.e., $\sum_{y=o,y\neq i}^{N_c-1}|\delta_{y-i}|^2 = \sum_{y=1}^{N_c-1}|\delta_{y-i}|^2$. Also, by Parseval's theorem we have $|\delta_0|^2 = 1 - \sum_{y=1}^{N_c-1}|\delta_y|^2$ [15]. Letting $\lambda = E\{|\delta_0|^2\}$ and $E_H = \sum_{i=0}^{N_c-1}E\{|H(i)|^2\}$, (16) becomes

$$E_r = \frac{E_s E_H(1-\lambda)}{N_c}(1 + \frac{L}{N_p}) + \frac{L(E_U+\sigma_N^2)}{N_p} \tag{18}$$

According to (18), it is known that E_r is determined by the transmit power E_s, the phase noise λ, the desired signal power E_U, and the noise power σ_N^2 for a N_c subcarriers OFDM system using N_p pilots. As shown in (17), the increase of the variance of phase noise α decreases λ, and thus increases the residual SI power E_r.

The power of SI before digital cancellation E_I, i.e., the power of residual SI after analog SIC, can be computed as $E_I = \frac{E_s E_H}{N_c}$. Substituting it into (18), the power of the residual SI $\mathbf{Y}_r$ after digital SIC becomes

$$E_r = E_I(1-\lambda)(1 + \frac{L}{N_p}) + \frac{L(E_U+\sigma_N^2)}{N_p} \tag{19}$$

With E_r and E_I computed, the digital SIC ability G defined in (9) is obtained as

$$G = 10\lg \frac{\gamma_{\mathrm{IN}} + 1}{\gamma_{\mathrm{IN}}(1-\lambda)(1+\frac{L}{N_p}) + \frac{L(\gamma_{\mathrm{SN}}+1)}{N_p} + 1} \quad (20)$$

where $\gamma_{\mathrm{IN}} = E_I/\sigma_N^2$ denotes the interference-to-noise ratio (INR), i.e., the power ratio of the received digital SI (after the analog SIC) and noise, and $\gamma_{\mathrm{SN}} = E_U/\sigma_N^2$ is the received desired signal-to-noise ratio (SNR).

4. NUMERICAL AND SIMULATION RESULTS

In Section 3, we have observed that the SIC ability G is influenced by several parameters, such as the variance α (which is determined by the oscillator's 3dB coherence bandwidth $f_{3\mathrm{dB}}$ and the sampling interval T_s), the INR γ_{IN} and the SNR γ_{SN}. In this section, we present some numerical and simulation results to show their impact on the digital SIC ability.

We consider an OFDM system with $N_c = 2048$ and $N_p = 64$, and the 64 pilots are uniformly inserted in the OFDM block. The SNR γ_{SN} is assumed as 10 dB, and the channel between the transmitter and the receiver is modeled a as Rayleigh fading channel.

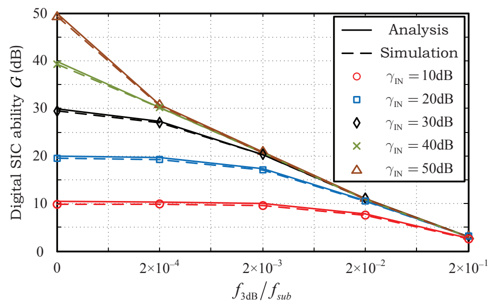

Fig. 2. Digital SIC ability with different f_{3dB}/f_{sub}.

Fig. 2 presents the digital SIC ability G in terms of the ratio of the oscillator's 3dB coherence bandwidth to the SI subcarrier spacing $f_{3\mathrm{dB}}/f_{sub}$. In Section 3, we know that the variance of phase noise α is related to this ratio, i.e., $\alpha = \frac{4\pi f_{3\mathrm{dB}}}{N_c f_{sub}}$, considering the SI bandwidth $B_W = 1/T_s$ and the subcarrier spacing $f_{sub} = B_W/N_c$. As shown in the figure, the simulation results match the corresponding analytical results well. For the scenario without phase noise, i.e., $f_{3\mathrm{dB}}/f_{sub} = 0$, the digital SIC ability G is approximately equal to INR γ_{IN}, demonstrating that the digital SIC almost reduces the SI to the noise floor. The tiny gap between G and γ_{IN} is caused by the estimation error of MLE. For the scenario with phase noise, G degrades with the increase of $f_{3\mathrm{dB}}/f_{sub}$ for any given γ_{IN}, and decreases faster for a larger γ_{IN}. For a typical value of $f_{3\mathrm{dB}} = 100$Hz [12] and INR is 40dB, the digital SIC could only reduce 11dB in the case of a 10 MHz OFDM SI signal with 2048 subcarriers, which will cause significant performance degradation of desired signal demodulation.

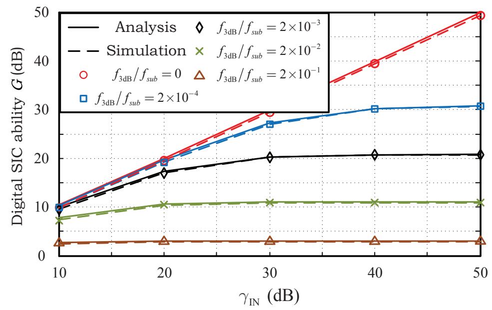

Fig. 3. Digital SIC ability with different INR γ_{IN}.

Fig. 3 presents the digital SIC ability G with different INR γ_{IN} ranging from 10 dB to 50 dB, and $f_{3\mathrm{dB}}/f_{sub}$ varying from 0 to 0.2. For the scenario without phase noise, i.e., $f_{3\mathrm{dB}}/f_{sub} = 0$, G increases linearly with γ_{IN}. For the scenarios with phase noise, G rises with γ_{IN}, and finally reaches an upper bound, which decreases with the increase of $f_{3\mathrm{dB}}/f_{sub}$.

5. RELATION TO PRIOR WORK

In this paper, we analysed the degradation effect of phase noise on the performance of the digital SIC scheme in wireless full duplex. This degradation effect was observed [6, 7] and also researched [4, 5] by Sabharwal's team. Compared with [4, 5], this work specifically focused on the impact of phase noise on the SI channel estimation in an OFDM-based full duplex radio, and thus derived the closed-form for the digital SIC ability, in terms of the INR and the ratio of the oscillator's 3dB coherence bandwidth to the SI subcarrier s-pacing.

6. CONCLUSION

In this paper, we considered the phase noise at both the transmitter and the receiver , which are modeled as independent Wiener processes, and analyzed their degradation effect on the performance of a common digital SIC scheme. The closed-form expression for digital SIC ability was derived in terms of the INR, the SI subcarrier spacing and the oscillator's 3dB coherence bandwidth. Theoretical analysis and simulations demonstrated that, as the ratio of the oscillator's 3dB coherence bandwidth to the SI subcarrier spacing increases, digital SIC performance will degrade, and the upper bound of the digital SIC ability will decrease. Thus, the phase noise has been proved to be a source of digital SIC performance degradation, and needs to be considered and compensated in full-duplex designs. The expressions and simulation results in this paper can be utilized in choosing an appropriate oscillator to meet the requirements of digital SIC for a given subcarrier spacing or bandwidth.

7. REFERENCES

[1] Y. Hua, P. Liang, Y. Ma, A. Cirik, and Q. Gao, "A method for broadband full-duplex mimo radio," *IEEE Signal Processing Letters*, vol. 19, pp. 793–796, Dec. 2012.

[2] R. Lopez-Valcarce, E. Antonio-Rodriguez, C. Mosquera, and R. Perez-Gonzalez, "An adaptive feedback canceller for full-duplex relays based on spectrum shaping," *IEEE Journal on Selected Areas in Communications*, vol. 30, pp. 1566–1577, Sep. 2012.

[3] J. Choi, M. Jain, K. Srinivasan, P. Levis, and S. Katti, "Achieving single channel, full duplex wireless communication," in *16th annual international conference on Mobile Computing and Networking*, 2010, pp. 1–12.

[4] A. Sahai, G. Patel, C. Dick, and A. Sabharwal, "Understanding the impact of phase noise on active cancellation in wireless full-duplex," in *2012 Conference Record of the 46th Asilomar Conference on Signals, Systems and Computers*, 2012, pp. 29–33.

[5] A. Sahai, G. Patel, C. Dick, and A. Sabharwal, "On the impact of phase noise on active cancellation in wireless full-duplex," *IEEE Trans. Vehicular Technology*, to appear.

[6] M. Duarte and A. Sabharwal, "Full-duplex wireless communications using off-the-shelf radios: Feasibility and first results," in *2010 Conference Record of the 44th Asilomar Conference on Signals, Systems and Computers*, 2010, pp. 1558–1562.

[7] M. Duarte, C. Dick, and A. Sabharwal, "Experiment-driven characterization of full-duplex wireless systems," *IEEE Trans. Wireless Communications*, vol. 11, pp. 4296–4307, Dec. 2012.

[8] M. Jain, J. Choi, T. Kim, D. Bharadia, S. Seth, K. Srinivasan, P. Levis, S. Katti, and P. Sinha, "Practical, real-time, full duplex wireless," in *17th annual international conference on Mobile Computing and Networking*, 2011, pp. 301–312.

[9] S. Hong, J. Mehlman, and S. Katti, "Picasso: Flexible rf and spectrum slicing," in *2012 conference on Applications, Technologies, Architectures, and Protocols for Computer Communication*, 2012, pp. 37–48.

[10] D. Bharadia, E. McMilin, and S. Katti, "Full duplex radios," in *2013 conference on Applications, Technologies, Architectures, and Protocols for Computer Communication*, 2012.

[11] E. Ahmed, A. Eltawil, and A. Sabharwal, "Rate gain region and design tradeoffs for full-duplex wireless communications," *IEEE Trans. Wireless Communication*, vol. 12, pp. 3556–3565, July 2013.

[12] T. Riihonen, P. Mathecken, and R. Wichman, "Effect of oscillator phase noise and processing delay in full-duplex ofdm repeaters," in *Signals, Systems and Computers (ASILOMAR)*, 2012, pp. 1947–1951.

[13] B. Day, A. Margetts, D. Bliss, and P. Schniter, "Full-duplex bidirectional mimo: Achievable rates under limited dynamic range," *IEEE Trans. Signal Processing*, vol. 60, pp. 3702–3713, July 2012.

[14] J. McMichael and K. Kolodziej, "Optimal tuning of analog self-interference cancellers for full-duplex wireless communication," in *Communication, Control, and Computing*, 2012, pp. 1–5.

[15] P. Mathecken, T. Riihonen, S. Werner, and R. Wichman, "Performance analysis of ofdm with wiener phase noise and frequency selective fading channel," *IEEE Trans. Communications*, vol. 59, pp. 1321–1331, May 2011.

[16] M. Morelli and U. Mengali, "A comparison of pilot-aided channel estimation methods for ofdm systems," *IEEE Trans. Signal Processing*, vol. 49, pp. 3065–3073, December 2001.

[17] S. Wu and Y. Bar-Ness, "Ofdm systems in the presence of phase noise: Consequences and solutions," *IEEE Trans. Communication*, vol. 52, pp. 1988–1996, November 2004.